*Journal of Interdisciplinary Mathematics*
ISSN: 0972-0502 (Print), ISSN: 2169-012X (Online)
Vol. 29 (2026), No. 6, pp. 1981–1990
DOI : 10.47974/JIM-2435

# Effect of dissipation on torsional wave propagation in an initially stressed visco-poroelastic sandy layer over a half-space

N. Radhika †
R. Archana Reddy §
*Department of Mathematics*
*School of Computer Science & Artificial Intelligence*
*SR University*
*Warangal 506371*
*Telangana*
*India*

G. Rajitha *
*Depatment of Mathematics*
*Sumathi Reddy Institute of Technology for Women*
*Warangal 506371*
*Telangana*
*India*

P. Latha Madhuri ‡
*Department of Mathematics*
*Kakatiya University*
*Warangal 506009*
*Telangana*
*India*

**Abstract**

The study evaluates how dissipation influences wave phenomena through a visco-poroelastic sandy layer and a visco-poroelastic semi-infinite half-space where initial stress exists. The model includes analysis of both poroelastic and viscoelastic characteristics together with detailed studies of solid-fluid phase connections in porous materials. The mathematical model relies on coupled equations that describe the mechanics of porous media, emphasizing the effects of viscosity and porosity on wave speed, attenuation, and dissipation. Influence

† *E-mail:* **radhikasathya99@gmail.com**
§ *E-mail:* **r.archanareddy@sru.edu.in**
* *E-mail:* **rajitha.akshu@gmail.com (Corresponding Author)**
‡ *E-mail:* **lathamadhuri25@gmail.com**

of several parameters including initial stress, viscosity, porosity, and dissipative effects on wave propagation are demonstrated numerically. Applications in Material Science, seismic exploration, Geotechnical Engineering can benefit from the findings, which offer valuable insights on how waves behave in porous media.

---

*Subject Classification: Primary 74JXX, Secondary 74J15.*

***Keywords:*** *Visco-poroelastic, Initial stress, Phase velocity, Attenuation, Wavenumber, Dissipation.*

## 1. Introduction

Investigation of transmission of waves in visco-poroelastic structures is valuable in the domains such as Rock Mechanics, Geophysics, and Civil Engineering, particularly, in Structural Engineering. The authors of the paper [1] present several mathematical arguments that highlight the importance that it is to incorporating viscoelastic effects into account. The viscoelastic analysis in structural design optimization has been examined by the authors of the following paper [2]. An analytical investigation of Love waves under initial stress in orthotropic granitic layers exists in [3]. Paper [4] addresses how viscosity, sandiness, and initial stress affect torsional waves. The findings of the study [5] summarized that there are no edge waves that exist in thick or thin isotropic plates when there is no incidence of initial stress. Chattaraj and Samal [6] discussed how the stiffness of reinforced materials affects wave characteristics. Considering the dispersion of waves through complex geological materials, particularly in exploration Geophysics and Rock Mechanics, several interconnected concepts are explored in the paper [7]. Paper [8] explores G-type wave propagation in fluid-saturated visco-poroelastic layers using Valeev's method. Employing Biot's theory of poroelasticity [9], Madhuri et al. [10] show that initial stress, porosity, and heterogeneity do have an influence on phase velocity. The proposed material modelling hypothesis advanced by Nowfal et al. [11], highlighted here, not only contributes to the knowledge base of scientific researchers and engineers, but also provides an assistive guide for opening up new applications in various industries. Kumar et al. [12] analyzed propagation of a plane wave surface on a nonlocal thermoelastic solid-half space that is isotopically homogeneous, and over an air half-space with a memory-dependent derivative and which has double porosity. This study [13] deals with the slanted magnetic field and rotation influence on viscoelastic fluid moving peristaltically via a porous medium in a tapered anisotropic slanted channel with variable viscosity and mixed convection heat transfer of the fluid inspected by Ramadhan and Jassim. The aforementioned papers did not investigate waves in the solids that are initially stressed visco-poroelastic sandy dissipated layers with visco-poroelastic dissipated half-spaces. This paper takes these characteristics into account and establishes the results accordingly. The results would have applications in destructive research, including subsurface material testing and seismic wave propagation.

**2. Geometry and Solution**

Consider an initially stressed viscoporoelastic sandy layer $(L_1)$overlying semi-infinite half-space $(L_2)$ in Cartesian coordinates. The origin locates on the boundary between the layer and the half space. Waves propagate downwards an axis, which is considered to be vertically downward, as depicted in Figure 1. From this figure, it is evident that the sandy layer and poroelastic half space are clearly occupying the spaces, $-H_1 \leq Z \leq 0$ and $Z \geq 0$, respectively. Following are the individual sub-sections where the solutions to each are provided.

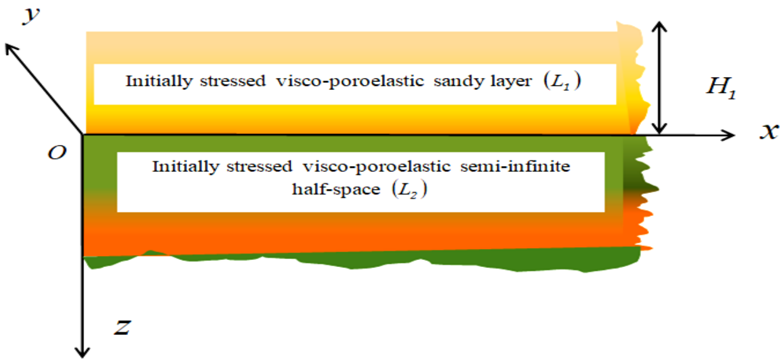


**Figure 1**
**Geometry of the problem.**

2.1 *Waves in Initially Stressed Visco-poroelastic Sandy Layer*

Suppose $u_1 = (u_1, v_1, w_1)$ and $U_1 = (U_1, V_1, W_1)$ are the displacement components of the solid and fluid of the initially stressed visco-poroelastic sandy layer$(L_1)$. For torsional vibrations, the displacements reduce to $v_1 = v_1(x, z, t)$,$u_1 = 0, w_1 = 0, and\ V_1 = V_1(x, z, t), U_1 = W_1 = 0$. The equations of motion in presence of dissipation reduce to

$$\frac{\partial \sigma_{12}}{\partial x} + \frac{\partial \sigma_{23}}{\partial z} - P_1 \frac{\partial \omega_{12}}{\partial x} = \frac{\partial^2}{\partial t^2}(\rho_{11} v_1 + \rho_{12} V_1) + b \frac{\partial}{\partial t}(v_1 - V_1),$$
$$0 = \frac{\partial^2}{\partial t^2}(\rho_{12} v_1 + \rho_{22} V_1) - b \frac{\partial}{\partial t}(v_1 - V_1). \tag{1}$$

In Eq. (1), $\sigma_{12}$ and$\sigma_{23}$are the stress components, $\omega_{12}$ are rotational components, $P_1, P_2$ are the initial stress, $\rho_{ij}$'s are mass coefficients, $b$ is dissipative coefficient. The stress components $\sigma_{ij}$and fluid pressure $S$are given by

$$\sigma_{ij} = 2\overline{N_1} e_{ij} + (Ae + Q\varepsilon)\delta_{ij},\ i, j = 1,2,3,$$
$$S = Qe + R\varepsilon. \tag{2}$$

From the above Eq.(2), $e_{ij}$'s are strain components, $\overline{N_1} = (N + \frac{N_1}{\eta_1}\frac{\partial}{\partial t}(i\omega t))$, $N$ is the shear modulus, $N_1$is the viscosity, $\eta_1$is sandy parameter, $\omega$

is frequency, $t$ is time, $A, Q, R$are all poroelastic coefficients. Now strain components $(e_{ij})$, rotational components $(\omega_{ij})$are given by,

$$e_{ij} = \frac{1}{2}\left(\frac{\partial u_i}{\partial x_j} + \frac{\partial u_j}{\partial x_i}\right), \quad \omega_{ij} = \frac{1}{2}\left(\frac{\partial u_i}{\partial x_j} - \frac{\partial u_j}{\partial x_j}\right), i, j = 1,2,3. \tag{3}$$

Consider $$v_1 = v_1(z)e^{i\,(\omega\, t - k\, x)}. \tag{4}$$

From Eqs. (1) to (4), the following differential equation is obtained

$$\frac{d^2 v_1(z)}{dz^2} - E^2 v_1(z) = 0. \tag{5}$$

In Eq. (5), $E^2 = g_1 + ig_2$,

$$g_1 = k^2\left(1 + \frac{\left(\frac{P_1}{2}\right)N}{N^2 + \left(\frac{N_1}{\eta_1}\right)^2\omega^2}\right) - \frac{1}{N^2 + \left(\frac{N_1}{\eta_1}\right)^2\omega^2}\left[N\omega^2\left(\rho_{11} - \frac{1}{b^2+\omega^2\rho_{22}^2}(2b^2\rho_{12} + b^2\rho_{22} - \omega^2\rho_{22}\rho_{12}^2)\right)\right] + \frac{1}{N^2 + \left(\frac{N_1}{\eta_1}\right)^2\omega^2}\left[\frac{\left(\frac{N_1}{\eta_1}\right)\omega^2 b}{b^2+\omega^2\rho_{22}^2}(b^2 - \omega^2\rho_{12}^2 - 2\omega^2\rho_{12}\rho_{22})\right],$$

$$g_2 = -k^2\left(\frac{\left(\frac{P_1}{2}\right)\left(\frac{N_1}{\eta_1}\right)\omega}{N^2 + \left(\frac{N_1}{\eta_1}\right)^2\omega^2}\right)\frac{1}{N^2 + \left(\frac{N_1}{\eta_1}\right)^2\omega^2}\left(\frac{N\omega b}{b^2+\omega^2\rho_{22}^2}[b^2 - \omega^2\rho_{12}^2 - 2\omega^2\rho_{12}\rho_{22}] - \left(\frac{N_1}{\eta_1}\right)\omega \left[\omega^2\rho_{11} - \frac{\omega^2}{b^2+\omega^2\rho_{22}^2}[2b^2\rho_{12} + b^2\rho_{22} - \omega^2\rho_{12}\rho_{22}]\right]\right).$$

The solution of Eq. (5) is

$$v_1 = (D_1 e^{g_1 z} + D_2 e^{g_2 z})e^{i(\omega\,\text{t-kx})} \tag{6}$$

In Eq. (6), here $D_1, D_2$ are arbitrary constants. The component of non-zero stress is

$$(\sigma_{yz})_{L_1} = \left(N + \frac{N_1}{\eta_1}i\omega\right)\,(D_1 g_1 e^{g_1 z} + D_2 g_2 e^{g_2 z})e^{i(\omega t - kx)}.$$

2.2 *Waves in Initially Stressed Visco-poroelastic Semi-infinite Half-space*

In lower visco-poroelastic layer $(L_2)$ and for torsional waves, displacements are $u_2 = 0, w_2 = 0,\ v_2 = v_2(x, z, t)$ and $U_2 = 0, W_2 = 0, V_2 = V_2(x, z, t)$. Equations of motion reduces to

$$\frac{\partial\sigma_{12}}{\partial x} + \frac{\partial\sigma_{23}}{\partial z} - P_2\frac{\partial\omega_{12}}{\partial x} = \frac{\partial^2}{\partial t^2}(\rho_{110}v_2 + \rho_{120}V_2) + b\,\frac{\partial}{\partial t}(v_2 - V_2),$$

$$0 = \frac{\partial^2}{\partial t^2}(\rho_{120}v_2 + \rho_{220}V_2) - b\frac{\partial}{\partial t}(v_2 - V_2). \tag{7}$$

From Eq. (7), $\sigma_{12}$ and $\sigma_{23}$are the stress components, $\omega_{xy}$ are rotational components, $P_2$ is the initial stress, and $\rho_{ij0}$ are mass coefficients.

$$\sigma_{ij} = 2\overline{N}_2 e_{ij} + (Ae + Q\varepsilon)\delta_{ij}, i, j = 1, 2, 3. \tag{8}$$

In Eq. (8), $\overline{N}_2 = (N_0 + N_{10}i\omega)$.

Consider $v_2 = v_2(z)e^{i(\omega t - kx)}$ is a solution of Eq. (7) (9)

From the Eqs. (7), (8), (3) and (9), the differential equation that results is as follows.

$$\frac{d^2 v_2(z)}{dz^2} - F^2 v_2(z) = 0. \tag{10}$$

In Eq. (10), $F^2 = g_3 + ig_4$.

The solution of Eq. (10) is,

$$v_2 = (D_3 e^{g_3 z}[cos(g_3 z) + i\, sin(g_4 z)] + D_4 e^{-g_3 z}[cos(g_3 z) - i\, sin(g_4 z)])e^{i(\omega\, \text{t-kx})} \tag{11}$$

In Eq. (11), $D_3, D_4$ are arbitrary constants. For lower layer as $z \to \infty$, the displacement component becomes

$$v_2 = (D_3 e^{g_3 z}[cos(g_3 z) + i\, sin(g_4 z)])e^{i(\omega\, \text{t-kx})} \tag{12}$$

$$g_3 = k^2\left(1 + \frac{\left(\frac{P_2}{2}\right)N}{N_0^2 + N_{10}^2\omega^2}\right) - \frac{1}{N_0^2 + N_{10}^2\omega^2}\left(N\omega^2\left[\rho_{110} - \frac{1}{b^2 + \omega^2\rho_{220}^2}(2b^2\rho_{120} + b^2\rho_{220} - \omega^2\rho_{220}\rho_{120}^2)\right]\right) + \frac{1}{N^2 + \left(\frac{N_1}{\eta_1}\right)^2\omega^2}\left[\frac{N_{10}\omega^2 b}{b^2 + \omega^2\rho_{220}^2}(b^2 - \omega^2\rho_{120}^2 - 2\omega^2\rho_{120}\rho_{220})\right],$$

$$g_4 = -k^2\left(\frac{\left(\frac{P_2}{2}\right)N_{10}\omega}{N_0^2 + N_{10}^2\omega^2}\right) - \frac{1}{N_0^2 + N_{10}^2\omega^2}\left(\frac{-N\omega b}{b^2 + \omega^2\rho_{220}^2}[b^2 - \omega^2\rho_{120}^2 - 2\omega^2\rho_{120}\rho_{220}] - N_{10}\omega\left[\omega^2\rho_{110} - \frac{\omega^2}{b^2 + \omega^2\rho_{220}^2}[2b^2\rho_{120} + b^2\rho_{220} - \omega^2\rho_{120}\rho_{220}]\right]\right).$$

The relevant stress component is

$$(\sigma_{yz})_{L_2} = \left(N + \frac{N_1}{\eta_1} i\omega\right)\, \mathrm{D}_3 e^{g_3 z}((g_3 + ig_4)\cos(g_4 z) + i(g_3 - ig_4)\sin(g_4 z))e^{i(\omega t - kx)}.$$

## 3. Boundary Conditions

(i) A stress-free boundary in contact with air is represented by the stresses vanishing at the free surface. It implies that no shear stress acts on this surface, allowing it to move or deform freely in response to the passing waves. At $z = -h_1$, the surface is free from any applied stress, i.e. $(\sigma_{\mathrm{yz}})_{L_1} = 0$.

(ii) The shear stresses at every contact between the poroelastic and viscoelastic layers are continuous, providing force equilibrium across the boundary. At $z = 0$, the stresses remain continuous, implying $(\sigma_{yz})_{L_1} = (\sigma_{yz})_{L_2}$.

(iii) The displacements are continuous at the same interfaces, providing medium kinematic compatibility. At $z = 0$ the displacement field is continuous, $v_1 = v_2$.

These specified boundary conditions produce a system of homogeneous equations with arbitrary constants $D_1, D_2, D_3$ leading to the following complex-valued frequency equation:

$$|a_{mn}| + i|b_{mn}| = 0, \qquad m, n = 1,2,3. \tag{13}$$

In Eq. (13), $a_{mn}$ and $b_{mn}$ are,

$$a_{11} = g_2 e^{-g_1 H_1} sin(g_2 H_1) + g_1 e^{-g_1 H_1} cos\ (g_2 H_1),$$
$$a_{12} = g_2 e^{g_1 H_1} sin(g_2 H_1) - g_1 e^{g_1 H_1} cos\ (g_2 H_1),$$
$$a_{13} = 0, a_{21} = g_1, a_{22} = -g_1, a_{23} = -g_3, a_{31} = 1 = a_{32}, a_{33} = -1,$$
$$b_{11} = -g_2 e^{-g_1 H_1} cos(g_2 H_1) + g_1 e^{-g_1 H_1} sin(g_2 H_1),$$
$$b_{12} = g_2 e^{g_1 H_1} cos(g_2 H_1) + g_1 e^{g_1 H_1} sin(g_2 H_1),$$
$$b_{13} = 0, b_{21} = g_2, b_{22} = -g_2, b_{23} = g_{20}, b_{31} = b_{32} = b_{33} = 0.$$

## 4. Particular Cases

**Case (i):** The problem minimizes to the poroelastic case when the viscous term is absent in presence of dissipative coefficient. In this case, the pertinent system of equations is

$$[A_{mn}]\ [D_m] = 0, \qquad m, n = 1,\ 2,\ 3. \tag{14}$$

$$A_{11} = g_2 e^{-g_1 H_1} + g_1 e^{-g_1 H_1}, A_{12} = g_2 e^{g_1 H_1} - g_1 e^{g_1 H_1}, A_{13} = 0,$$
$$A_{21} = g_1, A_{22} = -g_1, A_{23} = -g_3, A_{31} = A_{32} = 1, A_{33} = -1.$$

**Case (ii):** The fluid characteristics are neglected i.e., $\rho_{12} = \rho_{22} = 0$, $\rho_{11} = \rho, N_{10} = \mu$ and $\rho_{120} = \rho_{220} = 0$, $\rho_{110} = \rho'$, as an exceptional instance, the outcome of a purely elastic solid is obtained.

## 5. Numerical Results

The numerical approach taken into account two types of poroelastic solids: Mat-I, parameters taken from [14] and Mat-II from [15]. The dissipation coefficient $(b)$ is considered from [16]. Eq. (15) gives the phase velocity $(C_p)$ and attenuation $(Q_1^{-1})$ and to get these values, the following is used:

$$C_P = \frac{solution\ of\ real\ part\ of\ Eq.(14)}{Wavenumber}, Q_1^{-1} = \frac{2(solution\ of\ imaginary\ part\ of\ Eq.(14))}{solution\ of\ real\ part\ of\ Eq.(14)}. \tag{15}$$

The connection between phase velocity and wavenumber is derived from frequency equation. Phase velocity is calculated for various initial stress values against wavenumber using the bisection method in MATLAB, as shown in Figures 2-5. The physical parameter values are given in Table 1.

**Table 1**
**Material Parameters**

| Material Parameters | $A$ (Gpa) | $N$ (Gpa) | $Q$ (Gpa) | $R$ (Gpa) | $\rho_{11}$ (Kg/ m$^3$) | $\rho_{12}$ (Kg / m$^3$) | $\rho_{22}$ (Kg/m$^3$) | $N'$ (Gpa/m) |
|---|---|---|---|---|---|---|---|---|
| Mat-I | $0.443 \times 10^{10}$ | $0.276 \times 10^{10}$ | $0.076 \times 10^{10}$ | $0.032 \times 10^{10}$ | $1.926 \times 10^3$ | $-0.002 \times 10^3$ | $0.215 \times 10^3$ | $1.64 \times 10^{-3}$ |
| Mat-II | $0.306 \times 10^{10}$ | $0.922 \times 10^{10}$ | $0.013 \times 10^{10}$ | $0.063 \times 10^{10}$ | $1.903 \times 10^3$ | 0 | $0.226 \times 10^3$ | $1.00 \times 10^{-3}$ |

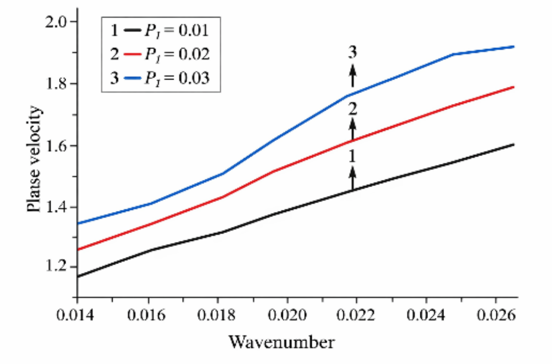


**Figure 2**

**Variation of wavenumber with phase velocity for distinct values of $(p_1)$ in the presence of dissipation.**

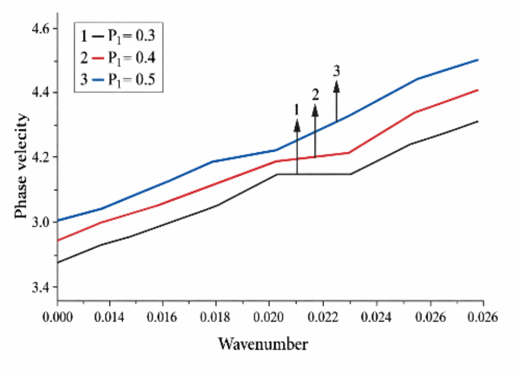


**Figure 3**

**Variation of wavenumber with phase velocity in absence of dissipation for distinct values of $(p_1)$.**

Figure 2 illustrates phase velocity with wavenumber for different initial stress values$(P_1)$, indicating an increase in phase velocity rising wavenumber in presence of dissipation. The correlation between wavenumber and phase velocity for various initial stress $(P_1)$ values, while maintaining a fixed value of initial stress$(P_2)$, is presented in Figure 3. This graph reveals that phase velocity increases with both wavenumber and initial stress values.

In this Figure 4, the dotted line indicates the trend without dissipation and remaining indicates the trend in presence of dissipation. This illustration demonstrates that phase velocity consistently rises with increasing of wavenumber, signifying a dispersive medium in which the phase velocity changes with wavenumber also in absence of dissipation a linear pattern emerges with phase velocity initially increasing, reaching maximum and then decreasing as wavenumber increases. If both initial stresses are zero, in the presence and absence of dissipation, the resulting trend exhibits linear behavior. The impact of attenuation is shown in Figure 5 for various values of wavenumber and initial stress$(P_1)$, which shows a trend as the wavenumber rises, so does the attenuation. This behavior can be explained by the fact that shorter wavelengths, which are more sensitive to the characteristics of the medium, including the amount of stress present, are associated with higher wavenumber.

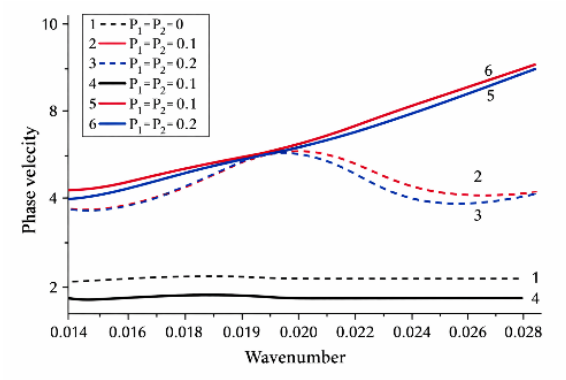


**Figure 4**
**Variation of wavenumber with phase velocity in the presence and absence of dissipation for fixed $(p_1)$ and $(p_2)$.**

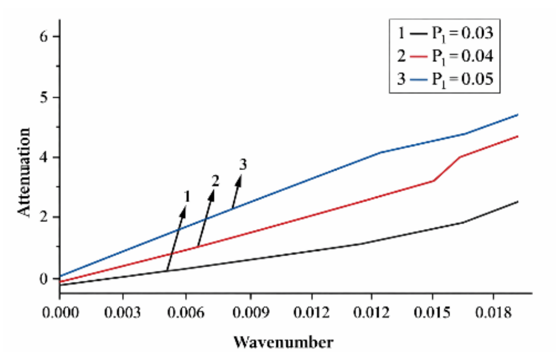


**Figure 5**
**Variation of wavenumber with attenuation for various initial stresses $(p_1)$ and fixed initial stress $(p_2)$ in the presence of dissipation.**

## 6. Conclusion

This study provides a detailed investigation of wave propagation in visco-poroelastic half-space with poroelastic sandy layer under initial stress. The findings reveal that initial stress and dissipation have a major impact on phase velocity and wave attenuation. This relationship shows how material stress, attenuation, and wave propagation interact in an elaborate way, and it implies that comprehending these relationships is essential to effectively modeling wave behavior in stressed media. Among the analysis main conclusions are:

(i) There was a significant impact on the attenuation characteristics when both initial stresses (($P_1$) and ($P_2$)) were present. High attenuation results from the medium's increased stiffness and resistance to wave motion as the initial stress rises.

(ii) Attenuation increases with wavenumber, especially when dissipation is present, according to the analysis. This is accordance with the hypothesis that shorter wavelengths are more susceptible to the characteristics of the medium, which are altered by stress and the material's viscoelasticity.

(iii) The study also highlights how dissipation contributes to wave attenuation. Increased attenuation results from the viscous nature of the medium, which causes energy loss to become more noticeable as dissipation increases.

## References

[1] S. Gupta, D. Majhi, S. Kundu, and S. K. Vishwakarma, "Propagation of Love waves in non-homogeneous substratum over initially stressed heterogeneous half-space," *Applied Mathematics and Mechanics*, vol. 34, no. 2, pp. 249–258 (2013).

[2] K. A. James and H. Waisman, "On the importance of viscoelastic response consideration in structural design optimization," *Optimization and Engineering*, vol. 17, no. 4, pp. 879–905 (2016).

[3] S. A. Ahmed and S. Abo-Dahab, "Propagation of Love waves in an orthotropic granular layer under initial stress overlying semi-infinite granular medium," *Journal of Vibration and Control*, vol. 16, no. 12, pp. 1845–1858 (2010).

[4] S. Gupta, M. Ahmed, S. Manna, and A. Pramanik, "Influence of initial stress and inhomogeneity on propagation of torsional type surface wave in a crustal layer," *International Journal of Geomechanics*, vol. 16, no. 4, Art. no. 06015012 (2016), doi: 10.1061/(ASCE)GM.1943-5622.0000562.

[5] K. A. Singh, A. Lakshman, and A. Chattopadhyay, "The plane waves at the edge of a uniformly pre-stressed fiber-reinforced plate," *Journal of Vibration and Control*, vol. 22, no. 10, pp. 2530–2541 (2016).

[6] R. Chattaraj and S. K. Samal, "Love waves in the fiber-reinforced layer over a gravitating porous half space," *Acta Geophysica*, vol. 61, no. 5, pp. 1170–1183 (2013).

[7] P. Kijanka and M. W. Urban, "Local phase velocity-based imaging of viscoelastic phantoms and tissues," *IEEE Transactions on Ultrasonics, Ferroelectrics, and Frequency Control*, vol. 68, no. 3, pp. 389–405 (2020).

[8] M. Venugopal, G. Rajitha, and P. M. Reddy, "G-type wave propagation in an initially stressed fluid saturated visco-poroelastic layer lying over heterogeneous poroelastic half space," *Mechanics of Solids,* vol. 57, no. 1, pp. 193–204 (2022).

[9] M. A. Biot, "Theory of propagation of elastic waves in a fluid-saturated porous solid. I. Low-frequency range," *The Journal of the Acoustical Society of America,* vol. 28, no. 2, pp. 168–178 (1956), doi: 10.1121/1.1908239.

[10] P. L. Madhuri, G. Rajitha, A. Sindhuja, and P. M. Reddy, "Initial stress and heterogeneity effects on torsional waves in dry sandy half-space between reinforced half-space and poroelastic medium," *Engineering Computations,* vol. 39, no. 5, pp. 1752–1767 (2021).

[11] S. H. Nowfal, G. R. K. Rao, V. Velmurugan, S. Sengan, R. K. Bommisetti, and P. Dadheech, "Advancing viscoelastic material modeling: Tackling time-dependent behaviour with fractional calculus," *Journal of Interdisciplinary Mathematics*, vol. 27, no. 2, pp. 307–316 (2024).

[12] R. Kumar, V. Gupta, V. Pathania, and M. S. Barak, "Response of memory to the imperfect fluid–double porous non-local thermoelastic solid interface," *Journal of Information and Optimization Sciences,* vol. 46, no. 5, pp. 1479–1503 (2025).

[13] M. S. Ramadhan and K. K. Jassim, "Impact of inclined magnetic field and rotation on peristaltic flow of viscoelastic fluid with variable viscosity," *Journal of Interdisciplinary Mathematics,* vol. 28, no. 3-A, pp. 729–740 (2025), doi: 10.47974/JIM-1968.

[14] I. Fatt, "The Biot-Willis elastic coefficients for a sandstone," *Journal of Applied Mechanics,* vol. 26, no. 2, pp. 296–297 (1959), doi: 10.1115/1.4012001.

[15] C. H. Yew and P. N. Jogi, "Study of wave motions in fluid-saturated porous rocks," *Journal of the Acoustical Society of America*, vol. 60, no. 1, pp. 2–8 (1976).

[16] G. Rajitha and P. M. Reddy, "Study of radial vibrations in thick walled hollow dissipative poroelastic spherical shell on elastic foundation," *Materials Physics and Mechanics,* vol. 44, no. 3, pp. 411–422 (2020).

*Received July, 2025*